Proceedings of the Institute of Acoustics

FLUID LOADING AND PIEZOELECTRIC ELEMENTS

P C Macey

PAFEC Ltd

1. Introduction

This paper considers methods of incorporating fluid loading and piezoelectric effects into finite element analyses. These two phenomena do not interact directly, only via the mechanical vibrations of the structure, and hence it is sufficient to consider separately how these effects are included.

The finite element method is a well established method for analysing structural vibrations. If the structure is surrounded by a compressible fluid then the surface vibrations will cause energy to be radiated away and it may be important to determine the surrounding pressure field. Furthermore, if it is a dense fluid, such as water, surrounding the structure then the pressure field will cause significant loading on the structure affecting the way it vibrates. In general the main effects are to introduce damping and increase the inertia of the structure, lowering the resonant frequencies.

Finite element methods cannot easily be used to model an infinite region of fluid. Boundary element methods are more suitable. For these only the wet surface of the structure needs to be modelled. Some simple fluid-structure interaction approximations permit the fluid degrees of freedom to be easily eliminated. Better methods lead to a complex dense set of equations for the fluid domain which must be solved in parallel with the structural equations.

Piezoelectric materials have a coupling between the mechanical deformation and the electric field. Modelling this with finite elements is relatively straightforward.

2. Basic Fluid Equations

Before considering fluid-structure interaction methods in detail it is necessary to consider some elementary fluid equations. Attention is restricted to an inviscid compressible fluid such that fluid particles vibrate with small amplitude and without any net flow.

The equation of motion of a small fluid particle is

$$\rho \ddot{\underline{u}} = - \underline{\nabla} P_t + \underline{g} \qquad (1)$$

where ρ is the density, $\underline{u}$ is the displacement, P_t is the pressure, $\underline{g}$ is the gravity vector and $\dot{}$ is used to denote temporal differentiation. Restricting attention to the oscillatory part of the pressure P, the excess above hydrostatic pressure, gives the equation

$$\rho \ddot{\underline{u}} = - \underline{\nabla} P \qquad (2)$$

The compressibility of the fluid is governed by the equation

$$\underline{\nabla} \cdot \underline{u} = - \frac{P}{K} \qquad (3)$$

where K is the bulk modulus.

Eliminating the displacements $\underline{u}$ between equations (2) and (3) gives

$$\nabla^2 P - \frac{1}{c^2} \ddot{P} = 0 \qquad (4)$$

where $c^2 = K/\rho$.

This is the wave equation, which occurs in many branches of physics. For steady state problems, vibrating at a fixed circular frequency ω the wave equation reduces to the Helmholtz equation,

$$\nabla^2 P + k^2 P = 0 \qquad (5)$$

where k is the wave number $(= \omega/c)$

In some applications excitation is applied to the fluid domain by a point source or a plane wave, coming from infinity. This incident wave is scattered by a submerged structure, which is caused to vibrate and radiate waves into the fluid domain. For some fluid-structure interaction methods it is useful to separate the pressure field into components as

$$P = P_I + P_R + P_r \qquad (6)$$

where P_I is the incident pressure, which would result if the structure were removed, P_R is the reflected pressure which would be the additional contribution caused by a rigid structure and P_r is the radiated pressure caused by the vibration of the structure's surface. The scattered pressure P_s is the sum of reflected and radiated fields.

3. Fluid Structure Coupling

In the following sections the problem of a structure vibrating in an infinite region of fluid is considered, see figure 1. It is assumed that the structure is modelled using the finite element method, as in figure 2. For the moment it will be assumed that the fluid region is modelled by a boundary element, as in figure 3, when only the fluid structure interface needs to be discretized. In order to couple these two regions together it is necessary to represent the effect of the surrounding pressure field as a set of nodal forces on the structural mesh and to compute the normal displacements at the nodes on the fluid mesh for a given structural deformation.

As derived in a previous lecture, the equations of motion for a finite element mesh is

$$[M]\{\ddot{u}\} + [S]\{u\} = \{F\} + \{F_f\} \tag{7}$$

Where $\{u\}$ is a column vector of structural displacements, $[M]$ and $[S]$ are the mass and stiffness matrices, $\{F\}$ is a vector of mechanical point forces and $\{F_f\}$ is a vector of forces due to the fluid. An expression for $\{F_f\}$ in terms of the nodal pressures on the fluid mesh can be derived by considering the work done by a virtual set of displacements on the fluid-structure interface Γ. Taking the normal $\underline{n}$ positive into the fluid, the work done by the fluid on the structure is given by

$$\begin{aligned} W &= \int_\Gamma - u_n P \, d\Gamma \\ &= - \{u\}^T \int_\Gamma [N_S]^T \underline{n}^T [N] \, d\Gamma \, \{P\} \\ &= - \{u\}^T [T]^T \{P\} \end{aligned} \tag{8}$$

where the coupling matrix $[T]$ is defined by

$$[T] = \int_\Gamma [N]^T \underline{n} [N_S] \, d\Gamma \tag{9}$$

and $[N]$ are the acoustic shape functions and $[N_S]$ are the structural shape functions. The work can also be expressed as $\{u\}^T \{F_f\}$. Since this is true for an arbitrary virtual displacement

$$\{F_f\} = - [T]^T \{P\} \tag{10}$$

To complete the coupling between the structural and fluid domains a transformation matrix [E] is required such that $[E]^T$ (u) gives the normal displacements on the fluid mesh.

The boundary element shape functions [N] are used for interpolating both pressures and normal displacements and hence an alternative way of computing the work done by a set of virtual displacements is as

$$\begin{aligned} W &= \int_\Gamma - u_n P \, d\Gamma \\ &= - \{u\}^T [E] \int_\Gamma [N]^T [N] \, d\Gamma \{P\} \\ &= - \{u\}^T [E] [A] \{P\} \end{aligned} \tag{11}$$

Where the area matrix [A] is defined by

$$[A] = \int_\Gamma [N]^T [N] \, d\Gamma \tag{12}$$

Hence one way of calculating [E] is by

$$[E] = [T]^T [A]^{-1} \tag{13}$$

Alternatively the normal displacement at a fluid node can be computed by interpolating the structural displacements with $[N_S]$ and using the local normal $\underline{n}$, and [E] can be constructed in a more direct manner. It is sometimes preferable to use equation (13) as this leads to symmetric equations for some fluid-structure interaction techniques.

4. Asymptotic Fluid-Structure Interaction Approximations

This section considers some approximate fluid-structure interation methods which are simple and can be easily implemented in finite element programs, but which only apply to restricted situations. In order to explain the range of applicability it is necessary to define the acoustic and structural wavelengths. For a steady state problem vibrating at frequency f ($= \omega/2\pi$), the acoustic wavelength is defined by

$$\lambda_{ac} = c/f \tag{14}$$

and is the distance between neighbouring peaks for a plane wave propagating in the fluid. The structural wavelength λ_{st} is the distance between neighbouring peaks on the deformed structural surface, see figure 4.

When the structure is vibrating such that

$$\lambda_{ac} << \lambda_{st} \tag{15}$$

The structure's surface is behaving locally in a one-dimensional manner, like a piston. In mathematical terms this is explained as follows. The wave equation (4) can be rewritten in the form

$$\frac{\partial^2 p}{\partial s_1^2} + \frac{\partial^2 p}{\partial s_2^2} + \frac{\partial^2 p}{\partial n^2} - \frac{1}{c^2}\frac{\partial^2 p}{\partial t^2} = 0 \qquad (16)$$

where S_1 and S_2 are tangential directions to the surface. The first two terms in equation (10) have order of magnitude $4\pi^2 P/\lambda_{st}^2$ and the last two are of order $4\pi^2 P/\lambda_{ac}^2$. Thus at high frequency, when equation (15) is satisfied, the wave equation reduces to

$$\frac{\partial^2 p}{\partial n^2} - \frac{1}{c^2}\frac{\partial^2 p}{\partial t^2} = 0 \qquad (17)$$

This one dimensional wave equation has the general solution

$$P = f(n + ct) + g(n - ct) \qquad (18)$$

The first term is the incident wave, travelling towards the structure, and the second term is the scattered wave. Hence the scattered wave must satisfy

$$\frac{\partial P_s}{\partial t} = - c \frac{\partial P_s}{\partial n} \qquad (19)$$

and thus, after using equation (2)

$$P_s = \rho c \dot{u}_{sn} \qquad (20)$$

the plane wave approximation is derived. If there is no incident wave, then this can be rewritten in matrix terms as,

$$\{P\} = \rho c \{\dot{u}_n\} \qquad (21)$$
$$= \rho c [E]^T \{\dot{u}\}$$

Where $\{u_n\}$ is the vector of normal displacements on the fluid mesh and $\{u\}$ are the structural displacements. Using equations (7), (10) and (13), the fluid degrees of freedom can be eliminated, giving

$$[M]\{\ddot{u}\} + [C]\{\dot{u}\} + [S]\{u\} = \{F\} \qquad (22)$$

where the damping matrix is given by

$$[C] = \rho c\ [E]\ [A]\ [E]^T \tag{23}$$

Thus the effect of the plane wave approximation is to introduce a fluid damping matrix into the structural equations. It must be remembered that this approximation is only valid for high frequency motions, see equation (15). For lower frequencies the plane wave approximation overdamps the solution.

The other extreme of low frequency motion, when

$$\lambda_{ac} >> \lambda_{st} \tag{24}$$

can be treated in a different manner. In this case the first two terms in equation (16) are dominant and so the wave equation reduces to Laplace's equation,

$$\nabla^2 P = 0 \tag{25}$$

Note that when the surrounding fluid is incompressible this equation is satisfied exactly. This can be solved for the pressure distribution outside some closed surface Γ, using boundary element techniques. From the divergence theorem it can be proved that

$$\epsilon P(\underline{x}) = \int_\Gamma \left(P(\underline{y}) \frac{\partial g}{\partial n_y} - g \frac{\partial P(\underline{y})}{\partial n_y}\right) d\Gamma(\underline{y}) \tag{26}$$

where $\epsilon = 1$ if $\underline{x}$ lies within the fluid, $\epsilon = 1/2$ if $\underline{x}$ is at a smooth point on the boundary and $\epsilon = 0$ if $\underline{x}$ lies within Γ, and g is the free space symmetric Green's function,

$$g(\underline{x}, \underline{y}) = 1 / (4\pi |\underline{x} - \underline{y}|) \tag{27}$$

The pressure P and its normal derivative $P_{,n}$ are interpolated using the same shape functions [N], and so equation (26) can be rewritten in a discretized form as,

$$\epsilon P(\underline{x}) - \sum_{i=1}^{n} \int_{P_i} \frac{\partial g}{\partial n_y} [N]\, d\Gamma\, \{P\} = - \sum_{i=1}^{n} \int_{P_i} g\, [N]\, d\Gamma\, \{P_{,n}\} \tag{28}$$

Where P_i is the i th patch on the boundary element and n is the number of patches. Taking $\underline{x}$ to be at one of the nodal points a linear equation relating the nodal pressures and pressure derivatives is obtained. Taking $\underline{x}$ to be at each nodal point in turn, a set of linear equations are obtained which can be written in matrix form as

$$[H]\{P\} = [G]\ \{P_{,n}\} \tag{29}$$

Using equation (2) this can be written in the form

$$[A]\ (P) = [M_f]\ (\ddot{u}_n) \tag{30}$$

where $[M_f]$ is known as the fluid mass matrix and is given by

$$[M_f] = \rho [A]\ [H]^{-1}\ [G] \tag{31}$$

DeRuntz and Geers [1] argue that only the symmetric part of $[M_f]$ is important. Using $[E]^T$ to relate displacements on the two meshes and from equations (7), (10) and (13),

$$([M] + [M_{ad}])\ \ddot{(u)} + [S]\ (u) = (F) \tag{32}$$

where the added mass matrix is defined by

$$[M_{ad}] = [E]\ [M_f]\ [E]^T \tag{33}$$

Thus the effect of a surrounding incompressible fluid is to increase the inertia of the structure without introducing any radiation damping.

The natural frequencies and mode shapes for a structure vibrating in an incompressible fluid can be determined by solving the eigenvalue problem

$$([S] - \omega^2\ ([M] + [M_{ad}]))\ (u) = (0) \tag{34}$$

Table 1 gives a comparison between an f.e/b.e solution for the mesh in figure 5 and a theoretical solution for the axisymmetric vibration modes of a spherical shell [2]. The spherical shell was 1m in radius, 0.02m in thickness and made of mild steel. The surrounding incompressible fluid was taken to have a density of 1000 kgm^{-3}.

Table 1. Natural Frequencies of a Spherical Shell

Number of meridional half waves	In Vacuo		In incompressible Fluid	
	FE	Theory	FE	Theory
1	1329.71	1392.55	511.62	511.56
2	614.05	605.59	383.06	382.10
4	768.61	765.43	521.26	519.70
6	824.16	818.10	601.70	596.99
8	893.76	877.83	687.49	674.22

5. Doubly Asymptotic Approximations

The fluid-structure interaction approximations of the last section are valid in certain frequency ranges. Doubly asymptotic approximations are formed by combining low and high frequency approximations to produce methods of greater applicability. The first order doubly asymptotic approximation (DAA1) is

$$[M_f]\ \dot{\{P\}} + \rho c\ [A]\ \{P\} = \rho c\ [M_f]\ \ddot{\{u_n\}} \qquad (35)$$

At low frequencies the second term dominates the left hand side and equation (35) degenerates to the virtual mass approximation. At high frequencies the first term is dominant and DAA1 becomes the plane wave approximation. DAA1 can be constructed from the virtual mass and plane wave approximations by using the method of matched asymptotic expansions. Felippa [3] has produced a second order doubly asymptotic approximation (DAA2) by combining a second order low frequency approximation, the corrected virtual mass approximation, with a second order high frequency approximation, the curved wave approximation. A simplified form of this is

$$[M_f]\ \ddot{\{P\}} + \rho c\ [A]\ \dot{\{P\}} + \rho c\ [\Omega]\ [A]\ \{P\} = \rho c\ [M_f]\ \dddot{\{u_n\}} + \rho c\ [\Omega]\ [M_f]\ \ddot{\{u_n\}} \qquad (36)$$

where

$$[\Omega] = \rho c\ [A]\ [M_f]^{-1} + c\ [\kappa] \qquad (37)$$

and $[\kappa]$ is a diagonal matrix of curvatures.

DAAs can be used for shock analysis. When an incident wave strikes a submerged structure there is initially high frequency vibration, but later on, when the structure is vibrating freely in the fluid, the behaviour is of a low frequency nature. DAA1 generally predicts initial response well, but overdamps and the solution is inaccurate at later times. Figure 6 illustrates the problem of a step incident wave striking a spherical shell. Huang [4] has considered this problem and produced a comparison of theoretical exact and theoretical DAA1 solutions which show the overdamping of the DAA. Figure 7 shows an f.e./b.e. mesh that was used to predict the response, and a comparison with Huang's theoretical DAA1 solution is given in figure 8.

The accuracy of the DAA2 method for harmonic problems is considered in figure 9 which reproduces a comparsion between a theorectical exact and a theoretical DAA2 solution for the problem of a spherical shell excited by harmonic end forces, shown in figure 10, taken from [2]. DAA2 works well apart from at resonances and anti-resonances. However, DAA2 can be used to accurately predict where resonances will occur.

To solve for structural and fluid response simultaneously using finite and boundary element methods, equations (7) and (36) can be combined to give

$$\begin{bmatrix} [Q_{ss}] & [Q_{sb}] \\ [Q_{bs}] & [Q_{bb}] \end{bmatrix} \begin{Bmatrix} \{u\} \\ \{P\} \end{Bmatrix} = \begin{Bmatrix} \{g_s\} \\ \{g_b\} \end{Bmatrix} \tag{38}$$

where

$$[Q_{ss}] = [S] - \omega^2 [M]$$

$$[Q_{sb}] = [T]^T$$

$$[Q_{bs}] = \rho c \, (i\omega^3 [M_f] [E]^T + \omega^2 [\Omega] [M_f] [E]^T)$$

$$[Q_{bb}] = -\omega^2 [M_f] + \rho c \, (i\omega [A] + [\Omega] [A]) \tag{39}$$

$$\{g_s\} = \{F\}$$

$$\{g_b\} = \{0\}$$

Once the component matrices $[M_f]$, $[A]$, $[S]$ etc have been calculated the equations in (38) can be rapidly formed, and if a staggered solution procedure can be used so the equations are efficiently solved then a rapid frequency scan can be made to determine the resonant frequencies. However, as noted above, the DAA2 method is not suitable for determining the resonant responses. This should be done using the exact formulations of the next section. These methods are slower in forming and solving the equations and are not as suitable for scanning the entire frequency range.

The problem of a spherical shell excited by harmonic point forces, shown in figure 10, was solved using the mesh of figure 5. The shell was taken to be made of mild steel and of thickness 0.02m. The surrounding fluid was taken to be water. A comparison of the computed and analytical solutions is given in figure 11.

6. Exact Boundary Element Techniques

The previous two sections have considered approximate boundary element methods for modelling fluid-structure interaction. Alternative techniques which are exact, within the accuracy of the discretization, are also available, but are generally more complicated, or have other difficulties.

Transient problems can be solved using Kirchhoff's retarded potential formulation [5]. This is a mathematical statement of Huygen's principle of wave propagation. However, its numerical implementation requires vast amounts of computer time and storage, and it is not considered in further detail here.

For harmonic problems "exact" methods are more widely used. The Helmholtz equation (5) can be solved directly using boundary element techniques. In this case the fundamental solution is

$$g\ (\underline{x},\ \underline{y}) = \exp\ (-ik\ |\underline{x} - \underline{y}|)\ /\ (4\pi\ |\underline{x} - \underline{y}|) \qquad (40)$$

Equation (26) still holds, and as in the solution of Laplace's equation, it can be discretized as equation (28), giving a linear equation relating the nodal pressures and normal pressure derivatives. To properly describe the fluid structure interaction m such equations are needed. These are usually obtained by taking $\underline{x}$ in turn to be at each of the m nodal degrees of freedom. This is known as the surface Helmholtz integral formulation and produces a matrix equation as in (29) except that [H] and [G] are now complex matrices.

An alternative, indirect approach, called the simple source formulation is based on representing the pressure in the external region as due to a distribution of point sources of density σ over the surface Γ .

$$P\ (\underline{x}) = \int_{\Gamma} \sigma\ (\underline{y})\ g\ (\underline{x},\ \underline{y})\ d\Gamma\ (\underline{y}) \qquad (41)$$

Letting $\underline{x}$ tend to a point on Γ gives the equation

$$P_{,n}\ (\underline{x}) = -\ \sigma\ /2 + \int_{\Gamma} \sigma(\underline{y})\ g_{,nx}\ d\Gamma\ (\underline{y}) \qquad (42)$$

Equations (41) and (42) can be discretized, interpolating the source density using the shape functions [N]. This gives a pair of matrix equations

$$\{P\} = [B]\ \{\sigma\} \qquad (43)$$

$$\{P_{,n}\} = [D]\ \{\sigma\} \qquad (44)$$

and by eliminating the source density σ a direct relationship between the pressure and its normal derivative is obtained.

Unfortunately the two above methods fail to work at certain frequencies. Copley [6] proves that these are the interior Dirichlet eigenvalues for the surface Γ . This is caused by a difficiency in the integral equation representation rather than any problem with the Helmholtz equation. Equation (26) fails to have a unique pressure distribution for a specified velocity, and hence pressure gradient distribution, causing the matrices [H] and [G] to be singular at these particular frequencies. For the simple source method, there is no suitable source density satisfying equation (41). However, the Helmholtz equation (5) does have a unique solution for the pressure distribution which satisfies the Sommerfield radiation condition, ie. decays to zero at infinity, for a given velocity distribution specified on Γ . On a finite precision computer the equations become ill-conditioned producing inaccurate results as the frequency approaches a critical frequency.

This is illustrated in figure 12 where equation (29) has been solved for the mesh of figure 13, modelling a uniformly pulsating sphere, by setting $P_{,n} = 1$ and comparing the computed pressure with the theoretical result.

A number of different methods are available for overcoming these difficulties. Schenck [7] has suggested a method called CHIEF (Combined Helmholtz integral equation formulation). The equations of the surface Helmholtz formulation are augmented with a few equations taking $\underline{x}$ interior to Γ and $\epsilon = 0$ in equation (26), and the resulting overdetermined system of linear equations are solved in a least squares manner. This works well provided the interior points chosen for $\underline{x}$ avoid the nodes of the interior eigenfunctions. Burton and Miller [8] have proposed an alternative method called CONDOR (composite outward normal derivative overlap relation). A complex linear combination of equation (26) and its normal derivative is used. Difficulty occurs in this method because of the highly singular integrals which need to be evaluated.

Once a boundary integral method has been chosen, giving an equation relating the pressure and its normal derivative, as in equation (29), this can be straightforwardly coupled to the finite element method, if Γ contains an elastic structure. From equation (2) the normal pressure derivatives can be expressed in terms of the structural displacements as

$$\{P_{,n}\} = \omega^2 \rho \ [E]^T \{u\} \tag{45}$$

and this leads to a set of equations as in (38) but where

$$[Q_{bs}] = -\omega^2 \rho \ [G] \ [E]^T$$

$$[Q_{bb}] = [H] \tag{46}$$

Once the equations have been solved and the pressure and velocity are known on Γ the pressure can be determined anywhere in the fluid using equation (26) and taking $\epsilon = 1$. Figures 14 and 15 show results for the vibrating spherical shell problem of figure 10 obtained by coupling the surface Helmholtz integral formulation to the finite element method for the mesh shown in figure 5.

The boundary element methods considered so far have all been local methods, ie. the variables to be solved for have been nodal pressure at specific points on Γ. Other more global methods exist, where an origin is chosen within Γ and the exterior pressure distribution is expressed as a sum of contributions from spherical harmonics [9]. The combination factors for these harmonics are solved for directly.

The methods described above have all assumed that the fluid surrounding the structure is linear and homogeneous.

If this is not true, eg. cavitation may occur in a transient analyses, or if there are variations in the density of the fluid near the structure, the methods may be adapted by using finite elements to model the nearby fluid [10]. Beyond this the fluid is again modelled by the appropriate boundary element techniques, and so assumed to be linear and homogeneous.

7. Piezoelectric Finite Elements

Piezoelectric materials have a coupling between the mechanical and electrical properties; deforming a piezoelectric crystal will cause a potential difference and vice versa. Thus it is necessary to solve the elastic and electrostatic equations simultaneously.

The virtual work density is

$$W = \underline{u}^T \underline{F} - \phi\, q \tag{47}$$

Where ϕ is the electric potential and q the charge density. The constitutive equations are

$$\begin{aligned} \sigma &= c\epsilon - e\,E \\ D &= e^T + \mathcal{E}\,E \end{aligned} \tag{48}$$

Where σ is the stress, ϵ the strain, E the electric field, D the flux density, c the elastic stiffness tensor, e the piezoelectric stiffness tensor and $\mathcal{E}$ the dielectric stiffness tensor. After applying the principle of virtual work the finite element equations can be derived as is done in ref [11],

$$\begin{bmatrix} [M_{uu}] & [0] \\ [0] & [0] \end{bmatrix} \begin{Bmatrix} \{\ddot{u}\} \\ \{\ddot{\phi}\} \end{Bmatrix} + \begin{bmatrix} [S_{uu}] & [S_{u\phi}] \\ [S_{\phi u}] & [S_{\phi\phi}] \end{bmatrix} \begin{Bmatrix} \{u\} \\ \{\phi\} \end{Bmatrix} = \begin{Bmatrix} \{F\} \\ -\{Q\} \end{Bmatrix} \tag{49}$$

where

$$\begin{aligned} [S_{uu}] &= \int_V [B_u]^T\, [c]\, [B_u]\, dV \\ [S_{u\phi}] &= \int_V [B_u]^T\, [e]\, [B_\phi]\, dV \\ [S_{\phi u}] &= \int_V [B_\phi]^T\, [e]^T\, [B_u]\, dV \\ [S_{\phi\phi}] &= \int_V [B_\phi]^T\, [\mathcal{E}]\, [B_\phi]\, dV \end{aligned} \tag{50}$$

and

$$[B_u] = \begin{bmatrix} \frac{\partial [N]}{\partial x} & 0 & 0 \\ 0 & \frac{\partial [N]}{\partial y} & 0 \\ 0 & 0 & \frac{\partial [N]}{\partial z} \\ \frac{\partial [N]}{\partial x} & 0 & \frac{\partial [N]}{\partial x} \\ \frac{\partial [N]}{\partial x} & \frac{\partial [N]}{\partial y} & 0 \end{bmatrix}$$

$$[B\phi] = \begin{bmatrix} \frac{\partial [N]}{\partial x} \\ \frac{\partial [N]}{\partial y} \\ \frac{\partial [N]}{\partial z} \end{bmatrix} \qquad (51)$$

[N] are the shape functions of the isoparametric element.

There are analogies between force and charge and between displacement and electric potential. In both cases the electrical quantity is one tensorial rank lower than the elastic quantity. The effect of an electrode can be modelled by repeating the electrical freedoms for nodes lying on some surface, by collapsing the rows and columns in the stiffness matrix. A connection to earth is modelled simply by restraining the appropriate electrical freedoms.

The electric freedoms can be eliminated by static condensation on equation (49) giving

$$[M^*] \{\ddot{u}\} + [S^*] \{u\} = \{F^*\} \qquad (52)$$

where

$$[M^*] = [M_{uu}]$$

$$[S^*] = [S_{uu}] - [S_{u\phi}] [S_{\phi\phi}]^{-1} [S_{\phi u}]$$

$$[F^*] = \{F\} + [S_{u\phi}] [S_{\phi\phi}]^{-1} \{Q\} \qquad (53)$$

Note that in order to perform this operation some electrical restraint must be applied, to ensure that $[S_{\phi\phi}]$ is not singular.

For harmonic vibrations at circular frequency equation (52) simplifies to

$$([S^*] - \omega^2 [M^*]) \{u\} = \{F^*\} \quad (54)$$

Natural frequencies and mode shapes can be found by setting $\{F^*\}$ to zero and solving the eigenvalue problem.

8. Conclusions

Techniques for applying fluid loading and incorporating piezoelectric effects in a finite element model have been considered.

For cases of low or high frequency vibration simplified approximate techniques are available which give added mass or added damping. More sophisticated approximate techniques can be used in the frequency domain to scan through and determine the resonances. Exact methods must be used for analysis near resonances if accurate results are to be obtained. However, boundary element methods based directly on the Helmholtz equation are computationally more expensive as all the boundary integrations must be performed for each frequency. All these methods , with the exception of the low frequency virtual mass approximation, complicate the solution procedure as the equations require complex arithmetic.

Examples have been presented for computations on spherical shells, where an analytical solution is available. These are not typical of transducers, but generally the effect of fluid loading will be greater for shell structures than for solid structures. Thus the methods described in the sections above are applicable to transducers.

Piezoelectric elements have been considered. These can be straightforwardly incorporated into a finite element system.

REFERENCES

[1] DeRuntz J.A. and Geers T.L.
"Added-mass computation by the boundary integral method"
Int. Jou. Num. Meth. Eng. Vol. 12 1978 pp 531-549

[2] Macey P.C.
"Acoustic and structure interaction problems using finite and boundary elements"
PhD thesis Nottingham University 1987

[3] Felippa C.A.
"Top down derivation of doubly asymptotic approximations for fluid-structure interaction analysis"
Proceedings of second international symposium on innovative numerical analysis for engineering sciences.
Montreal 1980

[4] Huang H.
"A qualitative appraisal of the doubly asymptotic approximation for transient analysis of submerged structures excited by weak shock waves"
NRL Memorandum Report 3135

[5] Huang H., Everstine G.C. and Wang Y.F.
"Retarded potential techniques for the analysis of submerged structures impinged by weak shock waves"
ASME AMD Vol 26 1977 pp 83-93

[6] Copley L.G.
"Fundamental results concerning integral representations in acoustic radiation"
Jou. Acoust. Soc. Am. Vol 44 No 1 1968 pp 28-32

[7] Schenck H.A.
"Improved integral equation formulation for acoustic radiation problems"
Jou. Acoust. Soc. Am. Vol 44 No 1 1968 pp 41-58

[8] Burton A.J. and Miller G.F.
"The applications of integral equation methods to the numerical solution of some exterior boundary-value problems"
Proc. Roy. Soc. London A323 1971 pp 201-210

[9] Waterman P.C.
"New formulation of acoustic scattering"
Jou. Acoust. Soc. Am. Vol 45 1969 pp 1417-1429

[10] Filippa C.A. and DeRuntz J.A.
"Finite element analysis of shock-induced hull cavitation"
Computer methods in applied science and engineering
Vol 44 1984 pp 297-337

[11] Allik H. and Hughes T.J.R.
"Finite element method for piezoelectric vibration"
Int. Jou. Num. Meth. Eng. Vol 2 1970 pp 151-170

FIGURE 1

elastic structure submerged
in infinite fluid

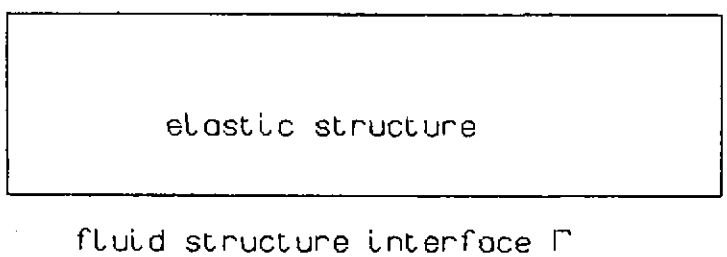

FIGURE 2

Finite element model of elastic structure

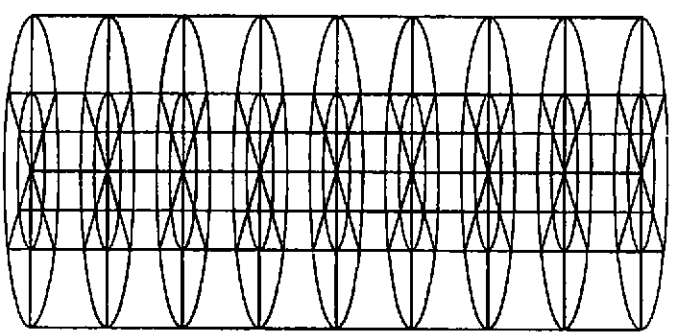

FIGURE 3

Boundary element mesh of external fluid

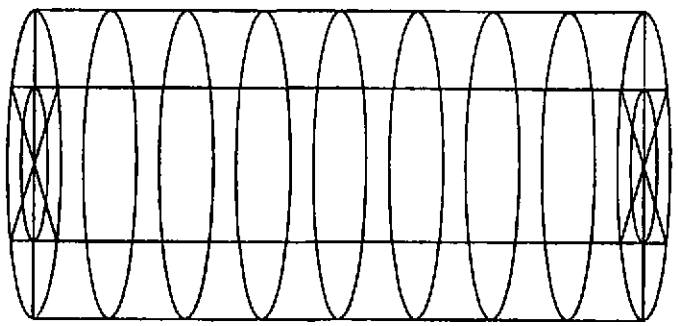

FIGURE 4

Acoustic and structural wavelengths

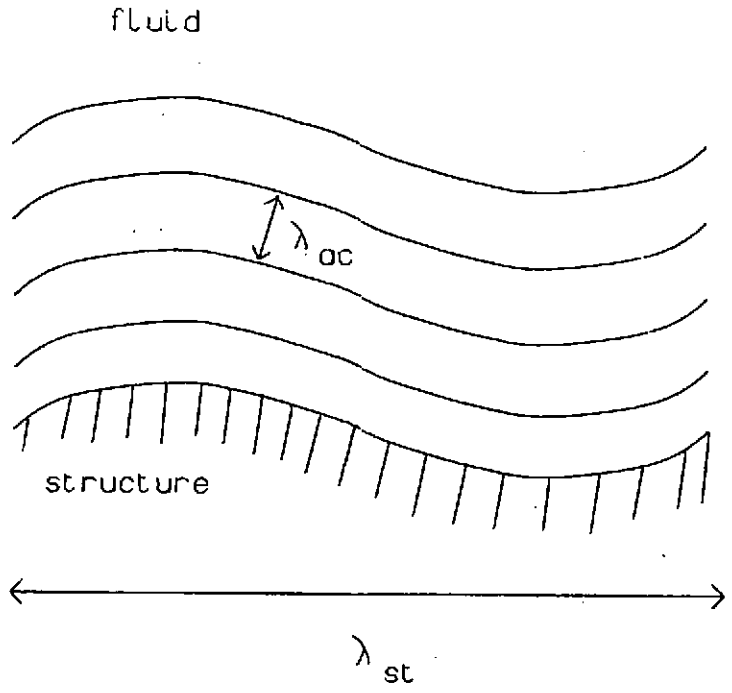

FIGURE 5

Fine mesh of eighth part of spherical shell

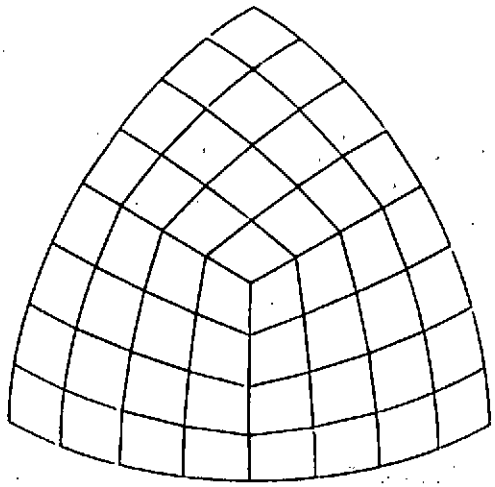

FIGURE 6

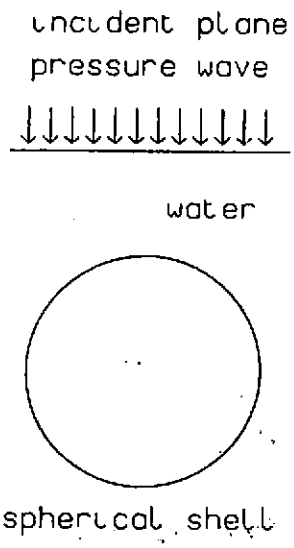

FIGURE 7

Mesh of quarter part of spherical shell

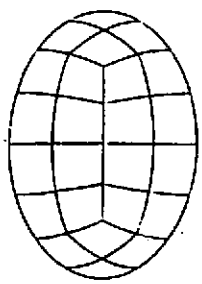

FIGURE 8

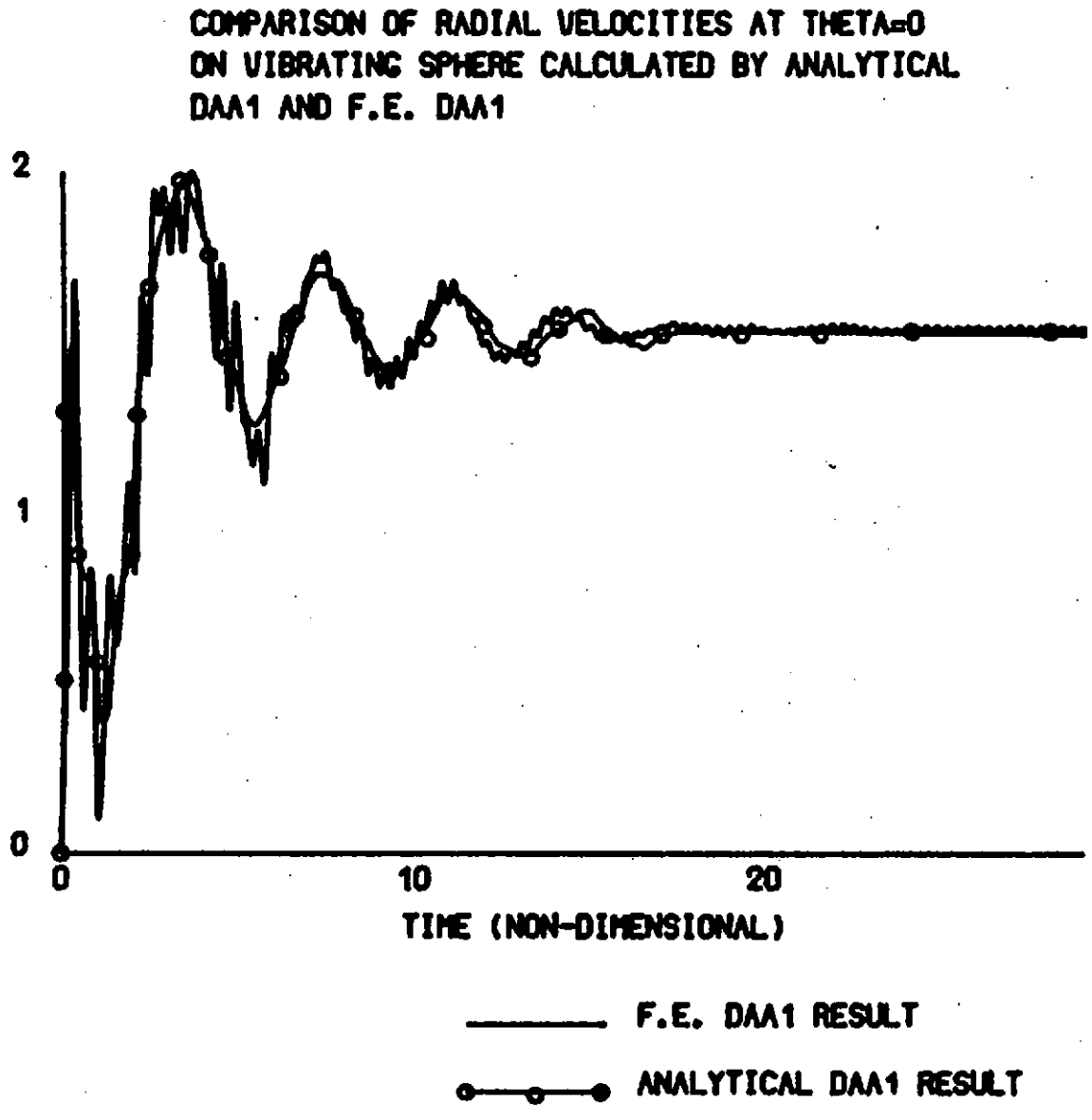
COMPARISON OF RADIAL VELOCITIES AT THETA=0
ON VIBRATING SPHERE CALCULATED BY ANALYTICAL
DAA1 AND F.E. DAA1
2
1
0
0
10
20
TIME (NON-DIMENSIONAL)
F.E. DAA1 RESULT
ANALYTICAL DAA1 RESULT

FIGURE 9 COMPARISON OF EXACT AND DAA2C RADIAL VELOCITY AT THE POINT OF EXCITATION FOR A SPHERICAL SHELL SUBMERGED IN WATER EXCITED BY HARMONIC END FORCES

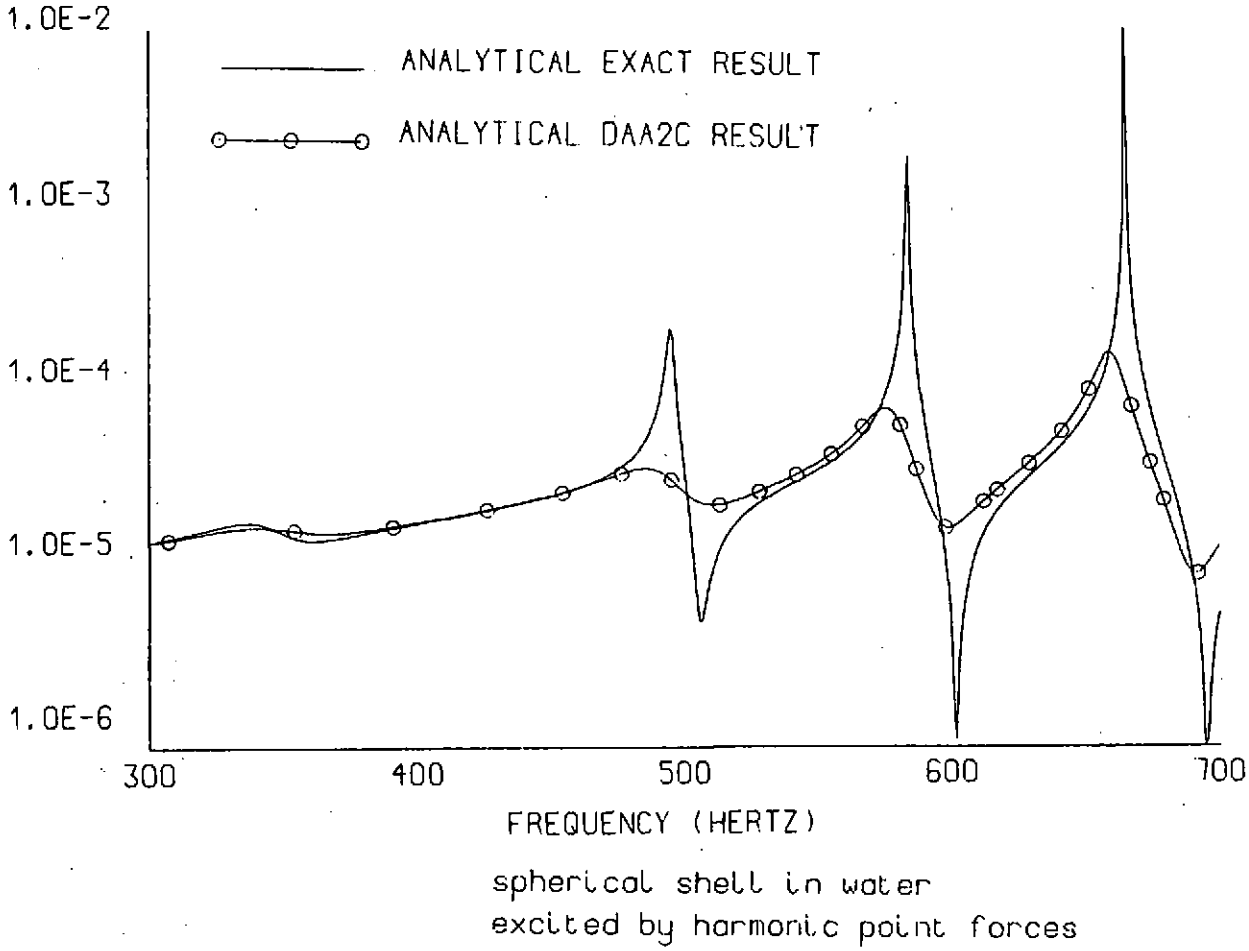

FIGURE 10

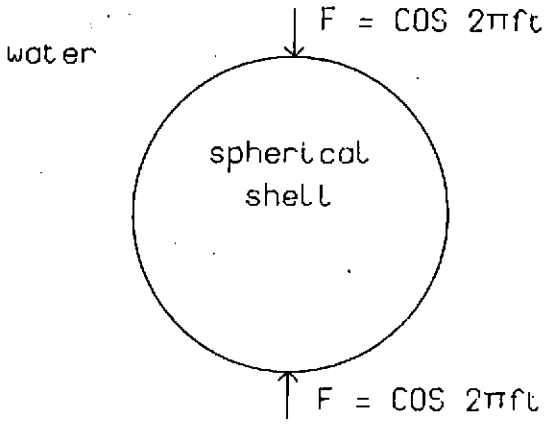

FIGURE 11

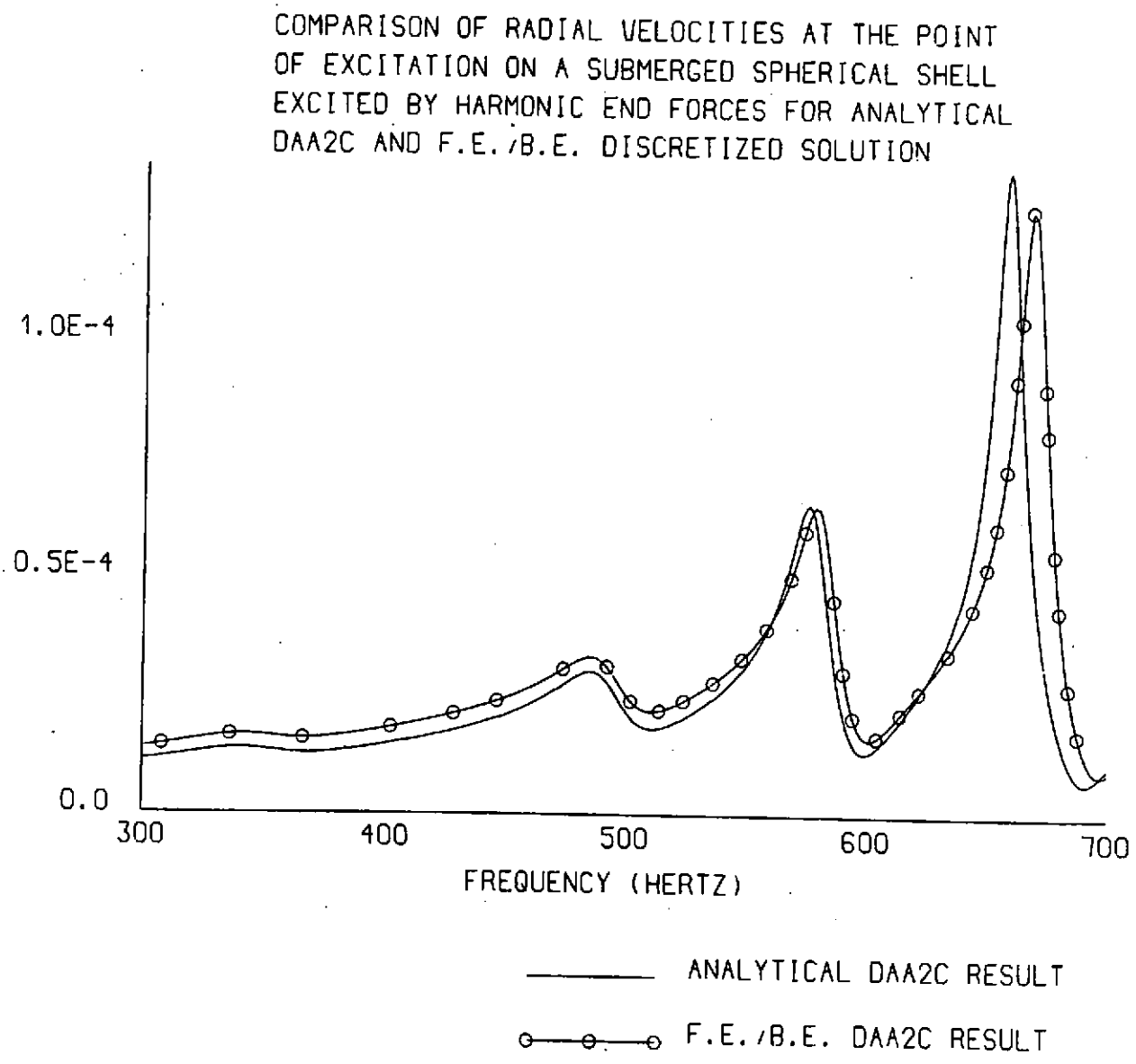
COMPARISON OF RADIAL VELOCITIES AT THE POINT OF EXCITATION ON A SUBMERGED SPHERICAL SHELL EXCITED BY HARMONIC END FORCES FOR ANALYTICAL DAA2C AND F.E./B.E. DISCRETIZED SOLUTION
1.0E-4
0.5E-4
0.0
300
400
500
600
700
FREQUENCY (HERTZ)
ANALYTICAL DAA2C RESULT
F.E./B.E. DAA2C RESULT

FIGURE 12

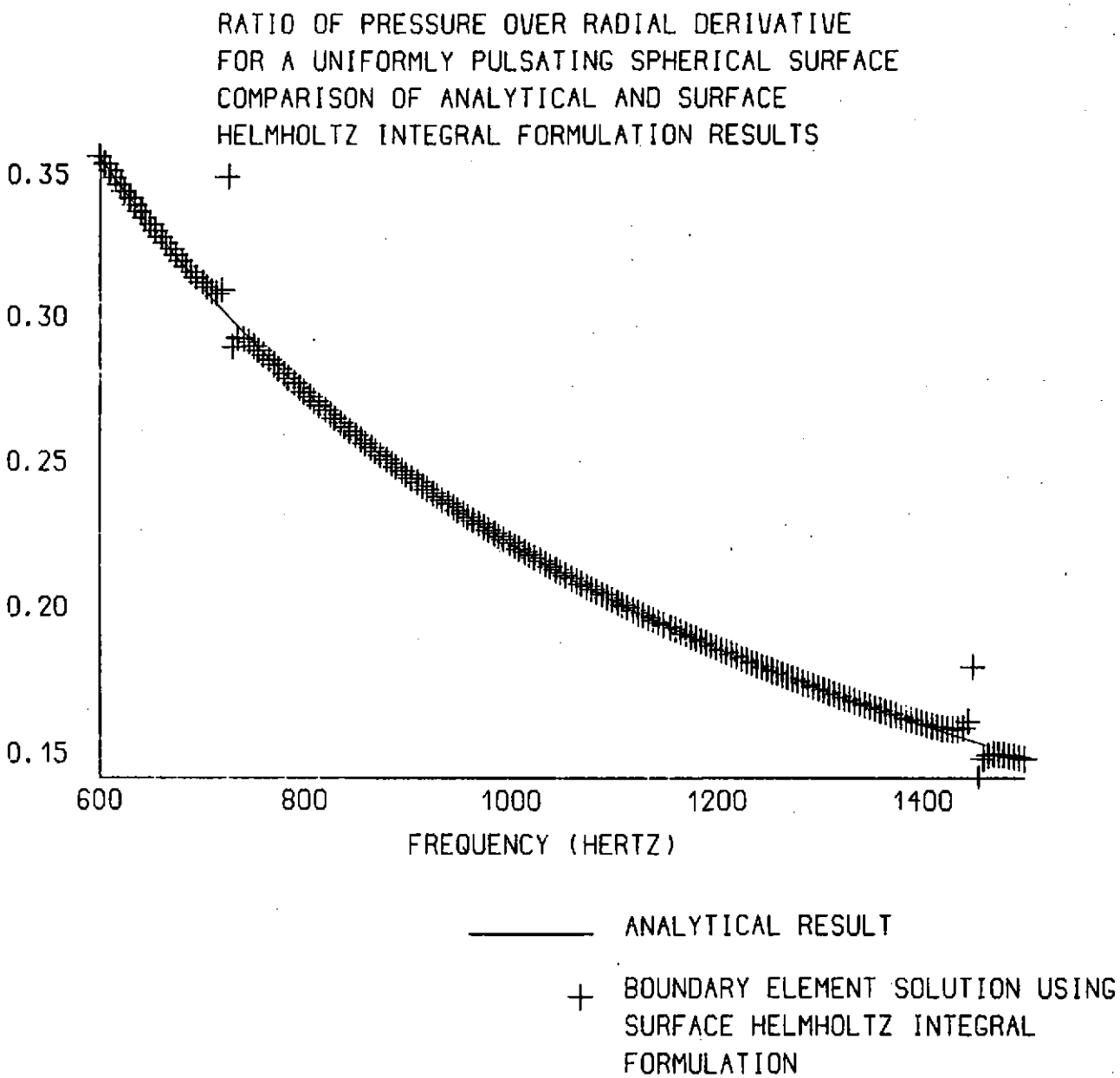
RATIO OF PRESSURE OVER RADIAL DERIVATIVE
FOR A UNIFORMLY PULSATING SPHERICAL SURFACE
COMPARISON OF ANALYTICAL AND SURFACE
HELMHOLTZ INTEGRAL FORMULATION RESULTS
0.35
0.30
0.25
0.20
0.15
600
800
1000
1200
1400
FREQUENCY (HERTZ)
ANALYTICAL RESULT
BOUNDARY ELEMENT SOLUTION USING
SURFACE HELMHOLTZ INTEGRAL
FORMULATION

FIGURE 13

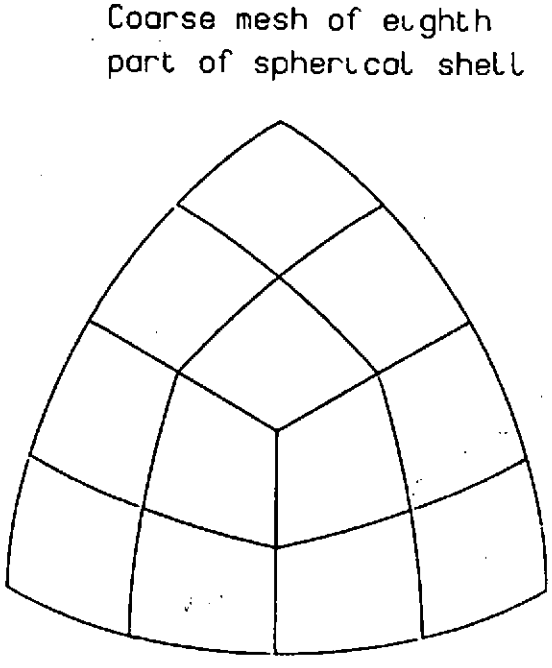

FIGURE 14

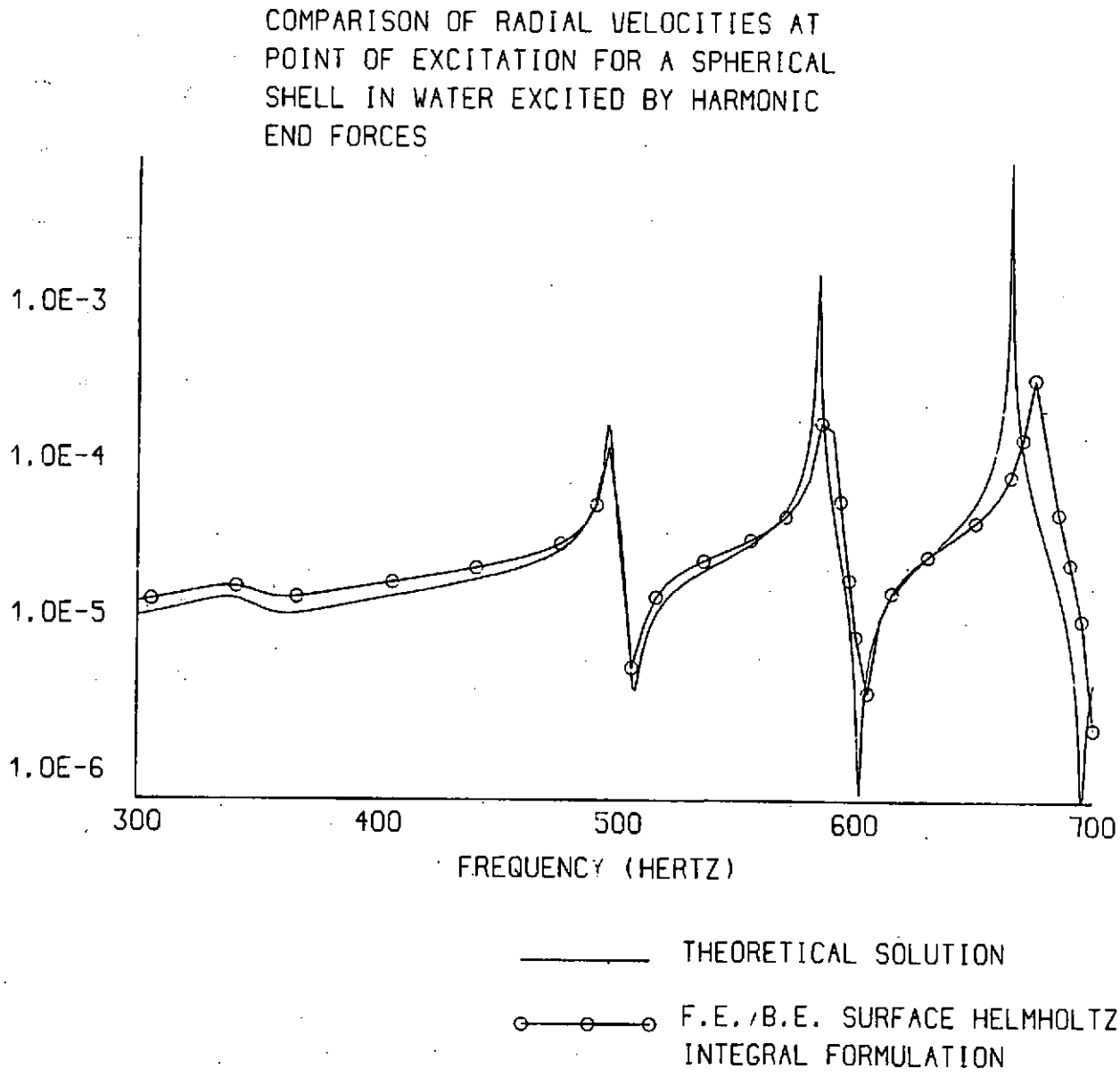
COMPARISON OF RADIAL VELOCITIES AT POINT OF EXCITATION FOR A SPHERICAL SHELL IN WATER EXCITED BY HARMONIC END FORCES
1.0E-3
1.0E-4
1.0E-5
1.0E-6
300
400
500
600
700
FREQUENCY (HERTZ)
THEORETICAL SOLUTION
F.E./B.E. SURFACE HELMHOLTZ INTEGRAL FORMULATION

FIGURE 15

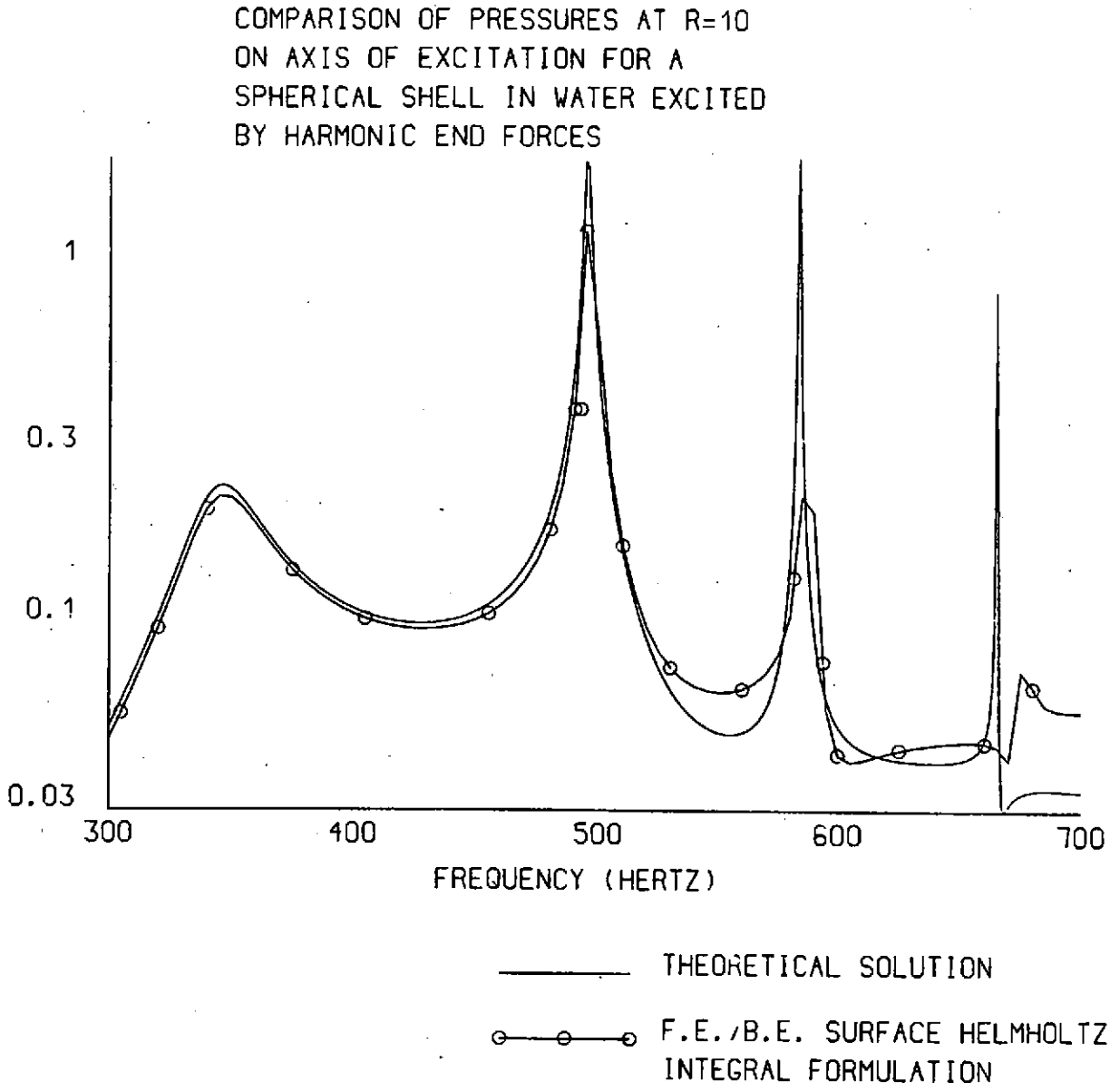
COMPARISON OF PRESSURES AT R=10
ON AXIS OF EXCITATION FOR A
SPHERICAL SHELL IN WATER EXCITED
BY HARMONIC END FORCES
1
0.3
0.1
0.03
300
400
500
600
700
FREQUENCY (HERTZ)
THEORETICAL SOLUTION
F.E./B.E. SURFACE HELMHOLTZ
INTEGRAL FORMULATION